Chapter 19
On the Origin of Mega-thrust Earthquakes

Kuvvet Atakan

Abstract Out of 17 largest earthquakes in the world since 1900 with magnitudes larger than 8.5, 15 of them occurred along convergent plate boundaries as mega-thrust events. Four of these catastrophic earthquakes have occurred during the last decade. The wealth of observational data from these events offer a unique opportunity for Earth Scientists to understand the underlying processes leading to the deformation in subductions zones, not only along the plate interface, but also in plate interiors in both the subducting slab and the overriding plate.

19.1 Introduction

Since the beginning of the twentieth century (i.e. 1900) there have been 17 earthquakes with magnitudes equal to or larger than 8.5 (Fig. 19.1). All of these earthquakes, except two, occurred due to rupture along the plate interface in different subduction zones around the Pacific and Indian oceans. Six of these occurred during the last decade, some of which with catastrophic consequences. Especially the largest of these, 2004 and 2005 Sumatra, Indonesia, 2010 Maule, Chile and the 2011 Tohoku-Oki, Japan earthquakes have provided new insights to the understanding of mega-thrust earthquakes and subduction zone deformation. There is now an unprecedented observational data from these events showing the details of the deformational processes in the convergent plate boundaries, not only along the plate interface of two colliding plates, but also within the plate interiors both on the overriding plate as well as the subducting slab (Table 19.1).

Mega-thrust earthquakes have some common characteristics. However, the wealth of data available for the latest events have highlighted the details of the rupture process and revealed significant differences. It became now clear that the physical properties of the plate interface in subduction zones are critical in the generation of the mega-thrust earthquakes. Understanding these processes in detail

K. Atakan (✉)
Department of Earth Science, University of Bergen, Allégt. 41, Bergen N-5007, Norway
e-mail: Kuvvet.Atakan@geo.uib.no

A. Ansal (ed.), *Perspectives on European Earthquake Engineering and Seismology*,
Geotechnical, Geological and Earthquake Engineering 39,
DOI 10.1007/978-3-319-16964-4_19

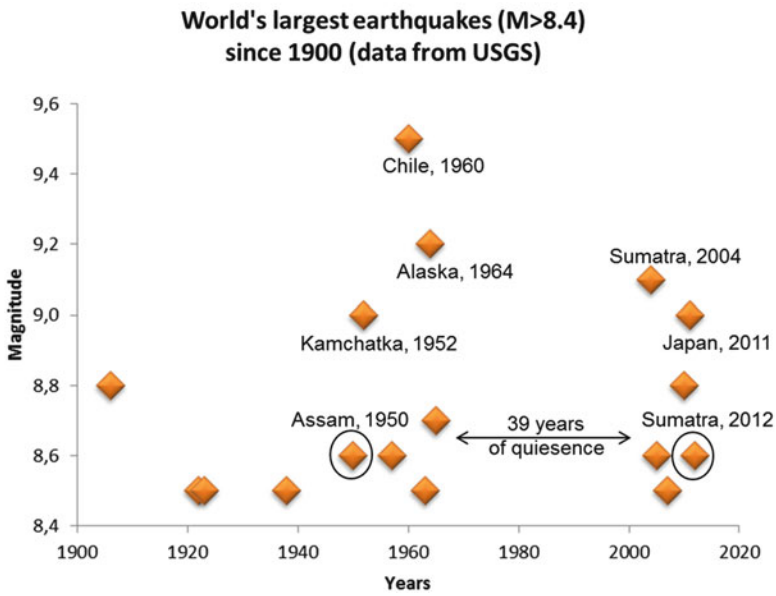

Fig. 19.1 World's largest earthquakes (M ≥8.5) since 1900 (data from USGS). Please note that the largest earthquakes have occurred in two clusters in time separated by 39 years. The two earthquakes, Assam 1950 and Sumatra 2012 earthquakes are not considered in this study as mega-thrust events. The 1950 Assam earthquake have occurred in a different tectonic setting with continent-continent collision, and the 2012 Sumatra earthquake was the largest ever recorded strike-slip faulting event which occurred along one of the fractures zones offshore northern Sumatra

requires multidisciplinary approaches synthesizing a variety of observational data combined with numerical and analogue modeling. Recent studies of the mega-thrust earthquakes have shown that there are methodological issues which may require revisiting some earlier wisdom, but they have also shown the capability of new promising techniques. In the following, we illustrate these challenging issues through various studies conducted on the latest earthquakes with a special emphasis on the 2011 Tohoku-Oki, Japan mega-thrust earthquake (M = 9.0).

19.2 Mega-thrust Earthquakes

Although there are far more very large earthquakes (M ≥8.0) that have occurred along the plate interface of various subduction zones which can be considered as mega-thrust events, in this study, we have restricted our definition of mega-thrust earthquakes to those that have magnitudes equal to or larger than 8.5. Among the 17 earthquakes since 1900 (Fig. 19.1), based on the data from USGS (USGS 2014), we consider 15 of them as mega-thrust events since the 1950 Assam earthquake

Table 19.1 List of world's largest earthquakes with M ≥8.5 in the period 1900–2014 (from USGS)

Date and time	Latitude	Longitude	Magnitude	Casualties	Region
1906/01/31 15:36	1.0	−81.5	8.8	1,000	Colombia-Ecuador
1922/11/11 04:32	−28.553	−70.755	8.5		Chile-Argentina Border
1923/02/03 16:01	54.0	161.0	8.5		Kamchatka
1938/02/01 19:04	−5.05	131.62	8.5		Banda Sea
1950/08/15 14:09	28.5	96.5	8.6	1,526	Assam-Tibet
1952/11/04 16:58	**52.76**	**160.06**	**9.0**		**Kamchatka, Russia**
1957/03/09 14:22	51.56	−175.39	8.6		Andreanof Islands, Alaska
1960/05/22 19:11	**−38.29**	**−73.05**	**9.5**	**1,655**	**Chile**
1963/10/13 05:17	44.9	149.6	8.5		Kuril Islands
1964/03/28 03:36	**61.02**	**−147.65**	**9.2**	**125**	**Prince William Sound, Alaska**
1965/02/04 05:01	51.21	−178.50	8.7		Rat Islands, Alaska
2004/12/26 00:58	**3.295**	**95.982**	**9.1**	**227,898**	**off the west coast of northern Sumatra**
2005/03/28 16:09	2.074	97.013	8.6	1313	Northern Sumatra, Indonesia
2007/09/12 11:10:26	−4.438	101.367	8.5	25	Southern Sumatra, Indonesia
2010/02/27 06:34:14	−35.846	−72.719	8.8	577	Offshore Maule, Chile
2011/03/11 05:46:23	**38.322**	**142.369**	**9.0**	**28,050**	**Near the East Coast of Honshu, Japan**
2012/04/11 08:38:37	2.311	93.063	8.6		off the west coast of northern Sumatra

All above earthquakes, except the 2012/04/11 event off the west coast of northern Sumatra, are mega-thrust earthquakes associated with the plate interface of a subduction process. 2012/04/11 event is the largest strike-slip earthquake ever recorded

have occurred in a different tectonic setting with continent-continent collision, and the 2012 Sumatra earthquake was the largest ever recorded strike-slip faulting event which occurred along one of the fractures zones offshore northern Sumatra. The remaining 15 events have all occurred along the various subduction zones in the Pacific and Indian Oceans. Their space/time correlations indicate that the largest of these earthquakes cluster in time. This is clearly shown in Fig. 19.1, with the two clusters in the time-periods 1950–1964 and 2004-present, separated by a quiescence period of 39 years. The most striking feature of these two clusters is that in the first cluster there were three mega-thrust events with M $\geq$9 and there were two M $\geq$9.0 in the second. Although it is tempting to suggest duration of approximately 10–15 years for these clusters with a rough repeat time of 40 years, statistically such conclusions are not warranted. This is mainly due to the fact that the total time of observation during the instrumental period is far too small and the two temporal clusters within 114 years cannot be generalized unless we have longer time series available. In spite of increasing evidence for mega-thrust events in the pre-historic period, assessing the occurrence of mega-thrust events during the historic and pre-historic period has some obvious limitations. In general the uncertainties of the source parameters increase significantly backwards in time. This however, should not undermine the importance of paleoseismological data which has proven useful in cases such as the subduction zone mega-thrust paleo-earthquakes of NW-US (1700, Cascadia earthquake; Satake et al. 1996) and in NE-Japan (869, Jogan earthquake; Minoura et al. 2001).

It is clear that the occurrence of these mega-thrust earthquakes is governed by global tectonics and the total seismic moment-budget associated with the plate convergence rates in the subduction zones (e.g. Pacheco and Sykes 1992; McCaffrey 2007). Nevertheless, their occurrence in time and space is highly dependent on the history of deformation in individual subduction zones and their internal segmentation within the arc. Despite this, there are some common characteristic that can be attributed to the mega-thrust earthquakes. These can be summarized as follows:

- All occur on subduction zones along the plate interface and cluster in time.
- All related to strong coupling along the plate interface, where the location and physical properties of the asperities are critical.
- Total slip is controlled by the size and the location of the strongest asperity (s) and if shallow, also controls the resulting tsunami size.
- Along-dip segmentation of the interface is observed and rupture may include the shallow trench-ward section.
- Along-strike segment boundaries are associated with large structural controls on the subducting plate (earlier sea-floor heterogeneities such as sea mount chains, ridges, fracture zones, etc.).
- All cause significant stress changes in the neighboring segments (including the outer-rise) and hence increase the likelihood of other mega-thrust events.
- All have clear signs of fore-shock activity and significant aftershock activity outside the main asperities.

Based on some of these common features there have been recent attempts to classify the different subduction zones and the associated mega-thrust earthquakes (e.g. Koyama et al. 2013). A simple classification based on three criteria, along-strike segment boundary, along-dip segmentation and the direction of collision (orthogonal or oblique), although useful to sort out some basic differences, still lacks the necessary details and hence forces one to think in terms of these end

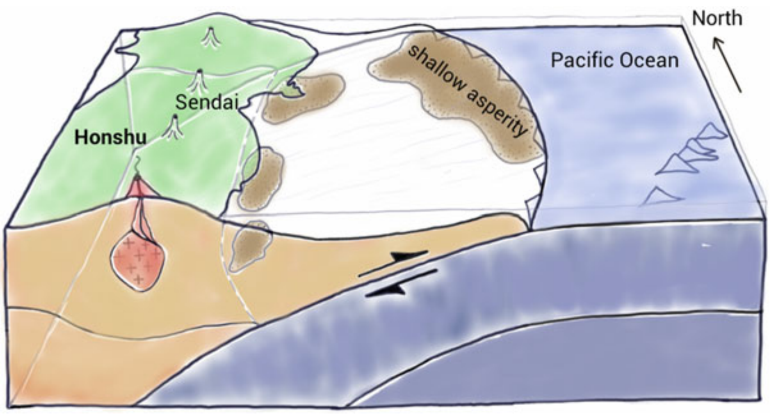

Fig. 19.2 Simplified sketch showing the cross-section along the Honshu, NE-Japan subduction zone. The approximate location of the asperities along the plate interface are shown with brown shaded areas. Note the sea-mount chain in the Pacific Ocean floor. See text for discussion

members only. However, understanding the subduction zone deformation requires a holistic approach to all controlling factors (Fig. 19.2).

A complete deformation cycle in a subduction zone starts with the inter-seismic period of strain accumulation due to the plate convergence, which in cases where there is strong coupling along the plate interface, results in internal deformation both in the overriding and subducting plates. In the overriding plate uplift occurs along the coastal areas of the island arc and inland regions whereas subsidence is seen towards the trench in the ocean-ward side. Both of these effects are the consequence of compressional forces due to locking of the plate interface. Observation of the sea-level changes in Sumatra and the response of the coral micro-atoll growth have demonstrated these long-term effects of overriding plate deformation (e.g. Zachariasen et al. 2000; Sieh et al. 2008). Similarly, in the subducting plate in the outer-rise region, compressional deformation occurs during the inter-seismic period, coupled with the down dip extension at depth giving rise to normal faulting deep intraplate events. Once the plate interface is ruptured through a mega-thrust earthquake (co-seismic deformation) the relaxation period following this favors the reversal of the forces acting in the same regions both in the overriding and subducting plates. Subsidence along the shore and inland regions accompanied by the uplift along the trench are typical for the overriding plate deformation. In the subducting plate the same structures that were reactivated as reverse faults now act as normal faults due to extension in the relaxation period (post-seismic deformation). There is off course processes both prior to the rupture of the plate interface (foreshock activity) and immediately after the mega-thrust earthquakes (aftershocks) which is part of the total deformation cycle. There are few examples that captures this total deformation cycle such as the triple earthquakes that have occurred along the central Kurile subduction zone in 1963 (M = 7.7), 2006 (M = 8.3) and 2007 (M = 8.1) (Raeesi and Atakan 2009).

19.3 Deformation Cycle in Subduction Zones

Understanding the total deformation cycle in subduction zones and the processes associated with it requires multidisciplinary approaches including a variety of observational data combined with analog and numerical modelling (Funiciello et al. 2013). In recent years indeed a wealth of observational data became available. These include,

- Structural data (conventional geology/geophysics)
- Petrophysical data (conventional petrology/geochemistry)
- Seismological data (conventional source parameters)
- Slip inversions based on seismological data for a broad-band of frequencies (backprojection methods for remote arrays etc.)
- Seismic tomography at a regional and detailed scales
- Seismic anisotropy
- Reflection/refraction profiles
- Potential field measurements (gravity, magnetics)
- Sattelite geodesy (GPS, InSAR, TEC)
- Borehole data
- Statistical data
- Paleoseismological data
- Tsunami data (run-up, modeling)
- Bathymetric surveys+DEM (digital elevation models at local scales)

Synthesizing such a variety of data brings along some methodological challenges as well. In the first place, it is necessary to realize the importance as well as the limitations of each data set before applying an appropriate method. Detailed studies of co-seismic slip-inversions through various data sets for the 2011 Tohoku-Oki, Japan mega-thrust earthquake, illustrate this problem very clearly. Following the earthquake of March 11, 2011 in Japan, there has been a number of co-seismic slip inversions published using tele-seismic data (e.g. Ammon et al. 2011; Ishii 2011; Lay et al. 2011; Koper et al. 2011; Wang and Mori 2011), strong-motion data (e.g. Ide et al. 2011; Suzuki et al. 2011), GPS data (e.g. Linuma 2011; Miyazaki et al. 2011; Ozawa et al. 2011; Pollitz et al. 2011) as well as tsunami data (e.g. Fujii et al. 2011; Saito et al. 2011). In addition to these there has also been joint inversions of seismological (teleseismic and strong-motion) and geodetic data (e.g. Koketsu et al. 2011; Yokoto et al. 2011; Yoshida et al. 2011; Kubo and Kakehi 2013). Common for all these inversion results is the shallow asperity with a large slip. In general there is a good agreement on the location of the shallow asperity among the various studies (seismological, GPS and tsunami wave data), where the maximum slip exceeds 40 m. When it comes to the details of the rupture there are significant differences in these inversion results. The main conclusion here is that slip inversions are non-unique and there is strong need for independent data which may help calibrating these. In other words, identifying the location of the strong asperities by multidisciplinary data sets seems critical. Independent evidence for the shallow asperity and the observed large slip came from the sea-bottom GPS measurements (Sato et al. 2011) and shallow seismic data (Kodaira et al. 2012) combined with cores from the borehole drilled at the tip of the sedimentary wedge (Chester et al. 2013).

The down-dip extent of the fault rupture is on the other hand, debated and some of the studies conclude that rupture propagated to the bottom of the contact zone. A number of inversions based on teleseismic data from large and dens arrays (US-array and the Stations from Europe) have revealed a strong short period radiation at deeper part of the rupture plane (e.g. Ide et al. 2011; Ishii 2011; Koper et al. 2011; Meng et al. 2011; Wang and Mori 2011). It is now understood that the slip associated with the shallow asperity was slow and lacking short-period radiation, whereas the deeper asperities produced strong short-period energy (Koper et al. 2011).

Apart from that, arguably, it can be said that the joint inversions smear out the slip distribution and a lot of details such as the short-period radiation at depth is not resolved (Meng et al. 2011). As such the common understanding that the joint inversions are better than individual data sets is questionable. The rupture complexity with a dynamic variation at various frequencies is better resolved by individual analysis of different data sets that are sensitive to these frequencies. The results from these individual studies, when combined together in a synthesis, seem to be a far better tool than the joint inversion results.

19.4 Rupture Preparation and Post-seismic Slip

Mega-thrust earthquakes along subduction zones are mainly controlled by the plate coupling along the interface. Some critical issues related to the degree of coupling are, the location of the strong and weakly coupled zones (asperities and their origin), role of sediments and fluids in coupling, down-dip limit of the coupled zone as well as coupling in the shallow zone close to trench. Regarding the latter the 2011 Tohoku-Oki earthquake has surprised many. Contrary to the common belief that the shallow part of the coupling along the trench is usually weak controlled by the loose sediments of the accretionary prism accompanied by the fluid interaction reducing the friction, more than 40 m of slip is observed along the trench. This very high slip along the trench was also crucial in the development of the following large tsunami wave.

The strongly coupled shallow asperity along the trench was manifested by the various co-seismic slip inversions as discussed earlier. It is also firmly confirmed by the offshore GPS measurements where significant slip was observed (Sato et al. 2011). The maximum horizontal slip measured was as high as 24 m almost 100 km away from the trench. The vertical uplift was as high as 3 m in the same area. The slip was also observed at the very tip of the trench through high resolution seismic data (Kodaira et al. 2012). Later, Chester et al. (2013) have shown the actual plate interface cutting through the contact between the pelagic sediments of the subducting plate and the sediments of the accretionary prism representing the overriding plate.

The rupture process had however started already with the onset of increased earthquake activity just at the periphery of this strong asperity at depth some weeks before the main rupture which culminated in a magnitude 7.5 earthquake at the deeper end of the shallow asperity on March 9, 2011. The static stress transfer from this event was probably the triggering mechanism for the main rupture on March 11, 2011. Such foreshock activity is not unique for the Tohoku-Oki earthquake, similar significant foreshock activity was previously documented in other plate interface thrust events (e.g. Raeesi and Atakan 2009) and more recently during the 2014 Iquique earthquake in northern Chile (Hayes et al. 2014).

Post-seismic slip is usually associated with extensive aftershock activity following the mega-thrust events. This was the case for the Tohoki-Oki earthquake where hundreds of aftershocks were registered in the following weeks after the main shock (Nishimura et al. 2011). The most striking feature of the aftershock sequences was their spatial concentration in areas outside the main asperities that had ruptured during the co-seismic slip. The largest of these aftershocks had a magnitude of 7.9 at the southernmost part of the plate interface off Boso, close to the Sagami trough in the south. In addition to the intensive aftershock activity along the plate interface, there has been also triggered seismic activity both in the overriding plate (Kato et al. 2011) and the subducting slab in the outer rise area such as the $M = 7.7$ earthquake (Lay et al. 2011). Such outer rise normal faulting events can be very large as was the case for the 1933 ($M = 8.4$) event further to the north. These events are the manifestation of the total deformation associated with the stress transfer from the main shock (Toda et al. 2011)

19.5 Segmentation of the Plate Interface

Physical conditions leading to the deformation in subduction zones depend on a variety of factors including:

- Direction and speed of the plate convergence.
- Differences in the rheology/composition of the two colliding plates.
- Age and density difference between and density variations within colliding plates.
- Physical/morphological/geological irregularities along the plate interface.
- The degree of coupling along the plate interface between the overriding plate and the subducting slab.
- Accumulated stress/strain.
- Fluid flow along the plate interface.
- Heat gradient and heat-flow.
- Melting process at the magma wedge. Mantle flow and circulations in the subduction system.

Although the total deformation is controlled by these factors, the physical and the morphological irregularities of the oceanic plate converging to the trench will in time have long term consequences in terms of the segmentation of the plate interface. Iquique ridge entering into the subduction zone in the border area between northern Chile and southern Peru is a good example for this (e.g. Pritchard and Simons 2006; Contreras-Reyes and Carrizo 2011; Métois et al. 2013). The strong coupling along this zone has previously been modelled (e.g. Métois et al. 2013; Chlieh et al. 2014) and is expected to produce large mega-thrust earthquakes probably larger than the recent Iquique event of 2014 ($M = 8.2$). Other sea-floor irregularities such as sea-mounts, fracture zones and ridges play thus an important role in the overall segmentation of the plate interface in various subduction zones.

19.6 Mapping Asperities

Once the segmentation of the interface is understood, the next critical issue is to find the location of the asperities. Inevitably, slip inversion of earthquakes constitutes an important contribution in this sense. However, there is a need for additional independent data to calibrate and verify the slip inversions as well as to find out more about the location of asperities in subduction zones where there are no recent large mega-thrust events in the latest instrumental period. One promising recent development is the use of satellite gravity data, GRACE in resolving the co-seismic gravity changes due to mega-thrust events (e.g. Tanaka and Heki 2014; Han et al. 2014). These new data opens new possibilities for detecting the location of asperities, because the repetitive slip along the same asperities of the plate interface causes mass dislocations. In the long-term, cumulative mass dislocations in the same part of the overriding plate will lead to permanent density changes. The accumulated density changes then leave an imprint on the overriding plate due to gravity (buoyancy forces) that change the degree of coupling along the plate interface. Cumulative effect of these variations should therefore be detectable as subtle deviatoric gravity changes parallel to the trench. These strongly coupled areas constitute the asperities that will slip in future large mega-thrust earthquakes. Mapping asperities by gravity data was first introduced by Song and Simons (2003), where trench parallel topography and gravity anomalies in the circum-Pacific region have revealed the strongly coupled areas along the plate interface. This was later modified (Raeesi and Atakan 2009; Raeesi 2009) to include also trench parallel Bouger anomaly.

Mapping asperities along the plate interface using these new techniques, if combined with detailed monitoring of seismological as well as geodetic changes in time with the recent observations regarding the short-term precursory phenomena such as total electron content (TEC) in the ionosphere (e.g. Liu et al. 2011; Tsugawa et al. 2011), may provide important opportunities to understand the deformation processes before the occurrence of the mega-thrust earthquakes.

19.7 Future Perspectives

In order to understand better the complex processes leading to mega-thrust earthquakes and the total deformation in subduction zones, future studies should focus on identifying the gaps for mega-thrust earthquakes as well as identifying the precursory phenomena in both long- and short-term. Following is a short list of research areas that may be helpful in this sense:

Identifying Gaps for Megathrust-Earthquakes

- Mapping the location of strongly coupled plate interface along subduction zones (GPS and stress modeling, stress transfer)
- Mapping the location and size of the largest asperities (Gravity, TPBA, seismic tomography)
- Mapping rupture areas of previous historical and instrumental mega-thrust earthquakes (historical accounts, slip distribution of previous instrumental mega-thrust earthquakes)
- Developing segmentation models for the subduction zones (mapping heterogeneities in the ocean-floor)

Identifying Precursory Phenomena

In the long-term:

- Monitoring overriding plate deformation (geodetic measurements of interseismic period through GPS, InSAR)
- Monitoring space/time variations of seismicity in the interseismic period (dense BB-station networks)

In the short-term:

- Identifying foreshock activity (detailed seismic monitoring)
- Identifying ionospheric disturbances (TEC measurements)

References

Ammon CJ, Lay T, Kanamori H, Cleveland M (2011) The rupture model for the great 2011 Tohoku earthquake. Earth Planets Space 63:693–696

Chester FM, Rowe C, Ujiie K, Kirkpatrick J, Regalla C, Remitti F, Moore JC, Toy V, Wolfson-Schwehr M, Bose S, Kameda J, Mori JJ, Brodsky EE, Eguchi N, Toczko S, Expedition 343 and 343 T Scientists, (2013) Structure and composition of the plate-boundary slip zone for the 2011 Tohoku-oki earthquake. Science 342:1208. doi:10.1126/science.1243719

Chlieh M, Mothes PA, Nocquet JM, Jarrin P, Charvisa P, Cisneros D, Fonta Y, Collot JY, Villegas-Lanzad JC, Rolandone F, Vallée M, Regnier M, Segovia M, Martin X, Yepes H (2014) Earth Planet Sci Lett 400:292–301. http://dx.doi.org/10.1016/j.epsl.2014.05.027

Contreras-Reyesa E, Carrizo D (2011) Control of high oceanic features and subduction channel on earthquake ruptures along the Chile–Peru subduction zone. Phys Earth Planet In 186:49–58. doi:10.1016/j.pepi.2011.03.002

Fujii Y, Satake K, Sakai S, Shinohara M, Kanazawa T (2011) Tsunami source of the 2011 off the Pacific coast of Tohoku, Japan earthquake. Earth Planets Space 63:815–820

Funiciello F, Corbi F, van Dinther Y, Heuret A (2013) Unraveling megathrust seismicity. EOS, Transactions. Am Geophys Union 94(51):497–498, 17 December 2013

Han SC, Sauber J, Pollitz F (2014) Broad-scale postseismic gravity change following the 2011 Tohoku-oki earthquake and implication for deformation by viscoelastic relaxation and afterslip. Geophys Res Lett. doi:10.1002/2014GL060905

Hayes GP, Herman MW, Barnhart WD, Furlong KP, Riquelme S, Benz HM, Bergman E, Barrientos S, Earle PS, Samsonov S (2014) Continuing megathrust earthquake potential in Chile after the 2014 Iquique earthquake. Nature 512:295–298. doi:10.1038/nature13677

Ide S, Baltay A, Beroza GC (2011) Shallow dynamic overshoot and energetic deep rupture in the 2011 Mw 9.0 Tohoku-oki earthquake. Science 332:1426. doi:10.1126/science.1207020

Ishii M (2011) High-frequency rupture properties of the Mw 9.0 off the Pacific coast of Tohoku earthquake. Earth Planets Space 63:609–614

Kato A, Sakai S, Obara K (2011) A normal-faulting seismic sequence triggered by the 2011 off the Pacific coast of Tohoku earthquake: wholesale stress regime changes in the upper plate. Earth Planets Space 63:745–748

Kodaira S, No T, Nakamura Y, Fujiwara T, Kaiho Y, Miura S, Takahashi N, Kaneda Y, Taira A (2012) Coseismic fault rupture at the trench axis during the 2011 Tohoku-oki earthquake. Nat Geosci 5:646–650. doi:10.1038/NGEO1547

Koketsu K, Yusuke Yokota Y, Nishimura N, Yagi Y, Miyazaki S, Satake K, Fujii Y, Miyake H, Sakai S, Yamanaka Y, Okada T (2011) A unified source model for the 2011 Tohoku earthquake. Earth Planet Sci Lett 310:480–487. doi:10.1016/j.epsl.2011.09.009

Koper KD, Hutko AR, Lay T, Ammon CJ, Kanamori H (2011) Frequency-dependent rupture process of the 2011 Mw 9.0 Tohoku earthquake: comparison of short-period P wave backprojection images and broadband seismic rupture models. Earth Planets Space 63:599–602

Koyama J, Yoshizawa K, Yomogida K, Tsuzuki M (2013) Variability of megathrust earthquakes in the world revealed by the 2011 Tohoku-oki earthquake. Earth Planets Space 64:1189–1198

Kubo H, Kakehi H (2013) Source process of the 2011 Tohoku earthquake estimated from the joint inversion of teleseismic body waves and geodetic data including seafloor observation data: source model with enhanced reliability by using objectively determined inversion settings. Bull Seismol Soc Am 103(2B):1195–1220. doi:10.1785/0120120113

Lay T, Ammon CJ, Kanamori H, Xue L, Kim MJ (2011) Possible large near-trench slip during the 2011 *M*w 9.0 off the Pacific coast of Tohoku earthquake. Earth Planets Space 63:687–692

Linuma T (2011) Coseismic slip distribution of the 2011 off the Pacific coast of Tohoku earthquake (M 9.0) estimated based on GPS data—was the asperity in Miyagi-oki ruptured? Earth Planets Space 63:643–648

Liu JY, Chen CH, Lin CH, Tsai HF, Chen CH, Kamogawa M (2011) Ionospheric disturbances triggered by the 11 March 2011 M9.0 Tohoku earthquake. J Geophys Res. 116:A06319. doi:10.1029/2011JA016761

McCaffrey R (2007) The next great earthquake. Science 315:1675–1676

Meng L, Inbal A, Ampuero JP (2011) A window into the complexity of the dynamic rupture of the 2011 Mw 9 Tohoku-Oki earthquake. Geophys Res Lett. 38:L00G07. doi:10.1029/2011GL048118

Métois M, Socquet A, Vigny C, Carrizo D, Peyrat S, Delorme A, Maureira E, Valderas-Bermejo MC, Ortega I (2013) Revisiting the North Chile seismic gap segmentation using GPS-derived interseismic coupling. Geophys J Int 194(3):1283–1294. doi:10.1093/gji/ggt183

Minoura K, Imamura F, Sugawara D, Kono Y, Iwashita T (2001) The 869 Jogan tsunami deposit and recurrence interval of large-scale tsunami on the Pacific coast of northeast Japan. J Nat Disaster Sci 23(2):83–88

Miyazaki S, McGuire JJ, Segall P (2011) Seismic and aseismic fault slip before and during the 2011 off the Pacific coast of Tohoku earthquake. Earth Planets Space 63:637–642

Nishimura T, Munekane H, Yarai H (2011) The 2011 off the Pacific coast of Tohoku earthquake and its aftershocks observed by GEONET. Earth Planets Space 63:631–636

Ozawa S, Nishimura T, Suito H, Kobayashi T, Tobita M, Imakiire T (2011) Coseismic and postseismic slip of the 2011 magnitude-9 Tohoku-Oki earthquake. Nature 475:373–376. doi:10.1038/nature10227

Pacheco JF, Sykes LR (1992) Seismic moment catalogue of large shallow earthquakes. Bull Seismol Soc Am 82(3):1309–1349

Pollitz FF, Bürgmann R, Banerjee P (2011) Geodetic slip model of the 2011 M9.0 Tohoku earthquake. Geophys Res Lett. 38:L00G08. doi:10.1029/2011GL048632

Pritchard ME, Simons M (2006) An aseismic slip pulse in northern Chile and along-strike variations in seismogenic behavior, J Geophys Res. 111:B08405. doi:10.1029/2006JB004258

Raeesi M (2009) Asperity detection along subduction zones. Unpublished PhD-thesis, University of Bergen, Department of Earth Science

Raeesi M, Atakan K (2009) On the deformation cycle of a strongly coupled plate interface: the triple earthquakes of 16 March 1963, 15 November 2006, and 13 January 2007 along the Kurile subduction zone. J Geophys Res. 114:B10301, 30. doi:10.1029/2008JB006184

Saito T, Ito Y, Inazu D, Hino R (2011) Tsunami source of the 2011 Tohoku-Oki earthquake, Japan: inversion analysis based on dispersive tsunami simulations. Geophys Res Lett. 38:L00G19. doi:10.1029/2011GL049089

Satake K, Shimazaki K, Tsuji Y, Ueda K (1996) Time and size of a giant earthquake in Cascadia inferred from Japanese tsunami records of January 1700. Nature 379:246–249

Sato M, Ishikawa T, Ujihara N, Yoshida S, Fujita M, Mochizuki M, Asada A (2011) Displacement above the hypocenter of the 2011 Tohoku-oki earthquake. Science 332:1395. doi:10.1126/science.1207401

Sieh K, Natawidjaja DH, Meltzner AJ, Shen CC, Cheng H, Li KS, Suwargadi BW, Galetzka J, Philibosian B, Edwards RL (2008) Earthquake supercycles inferred from sea-level changes recorded in the corals of West Sumatra. Science 322(5908):1674–1678. doi:10.1126/science.1163589

Suzuki W, Aoi S, Sekiguchi H, Kunugi T (2011) Rupture process of the 2011 Tohoku-Oki mega-thrust earthquake (M9.0) inverted from strongmotion data. Geophys Res Lett. 38:L00G16. doi:10.1029/2011GL049136

Tanaka Y, Heki K (2014) Long- and short-term postseismic gravity changes of megathrust earthquakes from satellite gravimetry. Geophys Res Lett 41:5451–5456. doi:10.1002/2014GL060559

Toda S, Lin J, Stein RS (2011) Using the 2011 M = 9.0 Tohoku earthquake to test the Coulomb stress triggering hypothesis and to calculate faults brought closer to failure. Earth Planets Space 63:1–6. doi:10.5047/eps.2011.05.010

Tsugawa T, Saito A, Otsuka Y, Nishioka M, Maruyama T, Kato H, Nagatsuma T, Murata KT (2011) Ionospheric disturbances detected by GPS total electron content observation after the 2011 off the Pacific coast of Tohoku earthquake. Earth Planets Space 63:875–879

USGS (2014) Largest earthquakes in the world since 1900. United States Geological Survey web-site: http://earthquake.usgs.gov/earthquakes/world/10_largest_world.php. Last accessed 6 Sept 2014

Wang D, Mori J (2011) Rupture process of the 2011 off the Pacific coast of Tohoku earthquake (Mw 9.0) as imaged with back-projection of teleseismic P-waves. Earth Planets Space 63:603–607

Yokota Y, Koketsu K, Fujii Y, Satake K, Sakai S, Shinohara M, Kanazawa T (2011) Joint inversion of strong motion, teleseismic, geodetic, and tsunami datasets for the rupture process of the 2011 Tohoku earthquake. Geophy Res Lett, 38:L00G21. doi:10.1029/2011GL050098

Yoshida Y, Ueno H, Muto D, Aoki S (2011) Source process of the 2011 off the Pacific coast of Tohoku earthquake with the combination of teleseismic and strong motion data. Earth Planets Space 63:565–569

Zachariasen J, Sieh K, Taylor FW, Hantoro WS (2000) Modern vertical deformation above the Sumatran subduction zone: paleogeodetic insights from coral microatolls. Bull Seismol Soc Am 90:897–913